Short Papers

Guided Mode Characteristics of Metal-Clad Planar Optical Waveguides Produced by Diffusion

SAMIR J. AL-BADER AND HUSSAIN A. JAMID

Abstract—**Analytical and numerical results for the guided mode characteristics of metal-clad planar waveguides produced by diffusion are developed. Values of the complex propagation constants are obtained numerically and are shown to be in good agreement with the analytical results. These give insight into how waveguide and material parameters determine the loss. Since the profile of the waveguide represents the variation of the refractive index of the diffused-channel waveguide with the depth dimension, the results obtained can be used to reduce the dimensionality of the diffused-channel waveguide and facilitate the application of the effective-index method.**

I. Introduction

The application of metallic overlays to planar waveguides is known to introduce modal loss that depends on the polarization (TE or TM) and on the refractive index variation of the waveguide [1]. It is known that TM mode attenuation is approximately an order of magnitude greater than TE mode attenuation. It is also known that the dependence of loss on mode order is a strong function of the index profile in graded-index waveguides. These characteristics give rise to a number of applications, such as mode and polarization filtering. Both step-index [2]–[4] and graded-index metal-clad waveguide types have been analyzed. The latter type has been considered with linear [5], exponential [6], and parabolic [7] graded-index profiles.

In this work, the metal-clad waveguide with a Gaussian-index profile is analyzed. This waveguide is particularly important in integrated optics because it is produced by one of the most frequently used methods of fabrication, namely the diffusion of metals, e.g. titanium, into $LiNbO_3$ or $LiTaO_3$ single crystals [8]. Detailed knowledge of the modal characteristics of the waveguide is essential for the purpose of controlling the fabrication process and realizing certain modal properties. Accurate analytical solutions of the propagation constants and the field modes are also important because this waveguide models the variation in the depth dimension (into the substrate) of the two-dimensionally varying refractive index of the diffused-channel waveguide. The application of the effective-index method, such as in [9], to reduce the dimensionality of the diffused-channel waveguide is facilitated by such solutions. However, because a closed-form solution of the wave equation for the waveguide with Gaussian profile has not been available, analysis must follow approximate methods. Perturbation theory in which the zero-order approximation is taken to be the solution of the parabolic profile has been used in [10]–[12]. Other approaches by which the waveguide has been analyzed have included the WKB method [13], [14] and other numerical methods [15]. In all these cases, only lossless media are considered, and although planar waveguides obtained by the diffusion of titanium into $LiNbO_3$ single crystals exhibit low modal loss [8], the presence of metallic overlays will introduce loss. The applications of interest to this work, namely mode and polarization filtering, depend fundamentally on loss. We develop a highly accurate closed-form description of the guided field by solving the wave equation directly. The results are applicable to cases where the metal cladding is replaced by a lossless dielectric of sufficiently low refractive index, such as air.

In Section II, we obtain the complex propagation constants and the waveguide modes by using a method due originally to Mullin [16]. The Gaussian function is expanded and powers through sixth order are retained. In Section III, an alternative, numerical scheme is used to calculate the complex propagation constants by integrating the wave equation for each guided mode and requiring that these modes satisfy the boundary conditions at the metal–dielectric interface. The efficiency of this scheme depends on a good initial estimate of the values of the propagation constants. These are taken from the results of the theory of Section II and adjusted in the integration scheme to ensure convergence. The feature of interest is that the adjustments are obtained by utilizing Muller's zero-finding algorithm [17]. It is noted that this scheme is applicable to cases where the index profile is an arbitrary function of the depth dimension. In Section IV, numerical results obtained from the methods of Sections II and III are compared and are contrasted with those obtained when only the first two terms of the Taylor series expansion of the Gaussian function are retained. It is shown that the two models yield similar results as the modes become well guided.

II. The Graded-Index Waveguide

A. Model

The refractive index distribution is taken to be

$$n^2(z) = n_2^2 + (n_1^2 - n_2^2)\, e^{-(z/a_z)^2} \qquad z > 0$$
$$= n_m^2 \qquad z < 0 \tag{1}$$

where n_1^2 and n_2^2 are the squares of the refractive indices of the surface and the bulk material, respectively, and n_m^2 corresponds to the metal cladding. All refractive indices, except that of the cladding, are real quantities. The parameter a_z is the diffusion depth and is related to the depth diffusion constant D_z by $a_z = 2(D_z t)^{1/2}$, where t is the diffusion time. In our analysis, we approximate (1) by

$$n^2(z) = n_2^2 + (n_1^2 - n_2^2)\left[1 - \left(\frac{z}{a_z}\right)^2 + \frac{1}{2}\left(\frac{z}{a_z}\right)^4 - \frac{1}{6}\left(\frac{z}{a_z}\right)^6\right] \qquad z > 0$$
$$= n_m^2 \qquad z < 0. \tag{2}$$

All complex refractive indices will be written in the form $n^2 = n'^2 + jn''^2$ where n'^2 represents the real part of n^2 and n''^2 represents the imaginary part.

Manuscript received October 1, 1986; revised February 4, 1987.

The authors are with the Department of Electrical Engineering, King Fahd University of Petroleum & Minerals, Dhahran, Saudi Arabia.

IEEE Log Number 8714116.

B. Theory

We assume that the refractive index increment

$$\frac{n_1^2 - n_2^2}{n_2^2} \ll 1.$$

The electromagnetic field of the waveguide must satisfy Maxwell's equations and both TE and TM waves under the above condition satisfy the wave equation

$$\frac{d^2\Psi}{dz^2} + k^2\left[n^2(z) - n_{\text{eff}}^2\right]\Psi = 0 \tag{3}$$

where, in order to be specific, Ψ represents H_z for TE modes and $n(z)E_z$ for TM modes. All field components are assumed to vary as $e^{-j(\omega t - \beta y)}$ with $\beta = kn_{\text{eff}}$ and k corresponds to free space. Accordingly, (3) is written in the form

$$\frac{d^2\Psi}{dz^2} + k^2\left[Q_0 + Q_2 z^2 + Q_4 z^4 + Q_6 z^6\right]\Psi = 0, \qquad z > 0 \tag{4}$$

where

$$\begin{aligned} Q_0 &= n_1^2 - n_{\text{eff}}^2 \\ Q_2 &= -\frac{n_1^2 - n_2^2}{a_z^2} \\ Q_4 &= \frac{n_1^2 - n_2^2}{2a_z^4} \\ Q_6 &= -\frac{n_1^2 - n_2^2}{6a_z^6}. \end{aligned} \tag{5}$$

We define the following quantities:

$$Q = Q_2 z^2 + Q_4 z^4 + Q_6 z^6 \tag{6}$$

$$R = \int_0^z Q^{1/2}\,dz = \frac{1}{2}Q_2^{1/2}z^2 + \frac{Q_4}{8Q_2^{1/2}}z^4 + \frac{4Q_2Q_6 - Q_4^2}{48Q_2^{3/2}}z^6 \tag{7}$$

$$\Omega_0 = k^2 + C_1 - \frac{q}{Q_2}C_2 \tag{8}$$

$$\Omega_1^2 = \frac{1}{4Q_2}\left(q - \frac{1}{2}C_2\right)^2 \tag{9}$$

$$q = k^2 Q_0 \tag{10}$$

$$C_1 = -\frac{5Q_6}{2Q_2^2} + \frac{327Q_4^2}{192Q_2^3} \tag{11}$$

$$C_2 = \frac{3Q_4}{4Q_2} \tag{12}$$

$$\zeta = 2\Omega_0^{1/4}R^{1/2}e^{-j\pi/4}. \tag{13}$$

The solution of (4) is [16]

$$\Psi = A(R/Q)^{1/4}D_\nu(\zeta), \qquad z > 0 \tag{14}$$

where D_ν are the parabolic cylinder functions, and

$$\nu = -\frac{1}{2} + j\Omega_1/\Omega_0^{1/2}. \tag{15}$$

The solution of the wave equation (3) in the metal cladding region is obtained by substituting n_m^2 for $n^2(z)$ and is given by

$$\Psi = Be^{\theta z} \tag{16}$$

where

$$\theta = k\left(n_{\text{eff}}^2 - n_m^2\right)^{1/2} \tag{17}$$

and B is an arbitrary constant.

C. TE and TM Mode Eigenvalue Equations

We use the solutions of the wave equation as given by (14) and (16), together with the continuity of tangential components at $z = 0$, to obtain the following eigenvalue equation:

$$\left[\frac{d\Psi}{dz}\Big/\Psi\right]_{z=0} = \rho\theta \tag{18}$$

where

$$\begin{aligned} \rho &= 1 && \text{for TE modes} \\ &= n_1^2/n_m^2 && \text{for TM modes} \end{aligned} \tag{19}$$

and Ψ is given by (14). This equation can be written as

$$\frac{d}{dz}\operatorname*{Lim}_{z\to 0}\ln(R/Q)^{1/4} + \frac{D_\nu'(0)}{D_\nu(0)}\left(\frac{d\zeta}{dz}\right)_{z=0} = \rho\theta \tag{20}$$

where the prime indicates differentiation with respect to the argument. By using (7), (8), and (13), it can be shown that (18) becomes

$$2^{1/2}\frac{D_\nu'(0)}{D_\nu(0)}\Omega_0^{1/4}Q_2^{1/4}e^{-j\pi/4} = \rho\theta. \tag{21}$$

We use the following relationships:

$$D_\nu(0) = \frac{\Gamma\left(\frac{1}{2}\right)2^{\nu/2}}{\Gamma\left(\frac{1-\nu}{2}\right)} \quad \text{and} \quad D_\nu'(0) = \frac{\Gamma\left(-\frac{1}{2}\right)2^{(\nu-1)/2}}{\Gamma(-\nu/2)}$$

to write (21) in terms of gamma functions in the following manner:

$$\frac{\Gamma(-\nu/2)}{\Gamma\left(\frac{1-\nu}{2}\right)} = \frac{-2\Omega_0^{1/4}Q_2^{1/4}e^{-j\pi/4}}{\rho\theta}. \tag{22}$$

The above equation is the eigenvalue equation whose roots give the complex values of the guided mode propagation constants of TE and TM modes. For the metals of interest, the right-hand side of (22) is a small quantity and decreases rapidly with increased diffusion depth. This suggests that solution of (22) may be sought where the real part of $\nu \approx 1, 3, \cdots$. It will be seen that with this approach (22) gives accurate results when compared with the results of the numerical scheme of Section III. In the following subsection, we develop analytical solutions for the real and imaginary parts of the propagation constants.

D. Solution of the Eigenvalue Equation

We first solve (15) for the variable q as follows:

$$q = \frac{1}{2}\left\{C_2\left[(2\nu+1)^2+1\right] + (2\nu+1)\sqrt{\left[(2\nu+1)^2+2\right]C_2^2 - 4Q_2\left(k^2 + C_1\right)}\right\}. \tag{23}$$

We write

$$\nu = \eta + j\delta \tag{24}$$

where $\eta \approx 1, 3, \cdots$ and δ is a small parameter. We designate the

real parts of q and Q_0 by q_r and Q_{0r}, respectively. Using (23) and (24) and noting that C_1, C_2, and Q_2 are real quantities, we obtain

$$Q_{0r} = \frac{1}{2k^2}\left\{ C_2\left[(2\eta+1)^2+1\right] + (2\eta+1)\sqrt{\left[(2\eta+1)^2+2\right]C_2^2 - 4Q_2\left(k^2+C_1\right)}\right\}. \quad (25)$$

The real part of n_{eff}^2 is determined from (25) and the first equation of (5) as follows:

$$n_{\text{eff}}'^2 = n_1^2 - Q_{0r} \quad (26)$$

while the imaginary part of n_{eff}^2 may be written in terms of Q_{0i}, the imaginary part of Q_0, as

$$n_{\text{eff}}''^2 = -Q_{0i}. \quad (27)$$

In order to determine the imaginary part of n_{eff}^2, we use (8), (9), (15), and (24) by writing

$$\eta + j\delta = -\frac{1}{2} + \frac{1}{2\sqrt{|Q_2|\Omega_{0r}}}\left[k^2(Q_{0r}+jQ_{0i}) - \frac{C_2}{2}\right]\left[1 - \frac{j\Omega_{0i}}{2\Omega_{0r}}\right] \quad (28)$$

where Ω_{0r} and Ω_{0i} are the real and imaginary parts of Ω_0, respectively. These are seen from (8) to be

$$\Omega_{0r} = k^2 + C_1 - k^2 Q_{0r} C_2/Q_2 \quad (29)$$

and

$$\Omega_{0i} = \frac{k^2 C_2 n_{\text{eff}}''^2}{Q_2}. \quad (30)$$

The fact that $n_{\text{eff}}''^2 \ll n_{\text{eff}}'^2$ has been used in (28).

In order to determine $n_{\text{eff}}''^2$, we use the method outlined in [7]. Utilizing a suitable expansion of the left-hand side of (22), this equation is written in the form

$$\frac{-2\Omega_0^{1/4}|Q_2|^{1/4}}{\rho\theta} = \frac{\Gamma\left(-\frac{\nu}{2}\right)\Gamma\left(1+\frac{\nu}{2}\right)}{\sqrt{\pi}} \cdot(1-\nu)\left(1+\frac{\nu}{2}\right)\left(1-\frac{\nu}{3}\right)\left(1+\frac{\nu}{4}\right)\cdots = \gamma + j\delta\sigma. \quad (31)$$

Using the complex expression for ν from (24) with $\eta = 1,3,\cdots$, the imaginary part of (31) to order δ gives

$$\delta = -\frac{2}{\sigma k}\Omega_{0r}^{1/4}|Q_2|^{1/4}\,\text{Im}\left[\frac{1}{\rho\left(n_1^2 - Q_{0r} - n_m^2\right)^{1/2}}\right] \quad (32)$$

where the values of σ for the first five modes are $\sqrt{\pi}$, 1.18194, 0.94530, 0.81026, and 0.72023, respectively. Note that only the real parts of Ω_0 and Q_0 are used since their imaginary parts are very small and that the properties of the metal are dominant in the quantity within the square brackets. By using (30) and the imaginary part of (28), the solution of $n_{\text{eff}}''^2$ is found to be

$$n_{\text{eff}}''^2 = \frac{4\left(|Q_2|\Omega_{0r}\right)^{3/4}}{k^3\sigma\left[1+\left(k^2Q_{0r}-\frac{C_2}{2}\right)\left(\frac{C_2}{2\Omega_{0r}Q_2}\right)\right]} \cdot \text{Im}\frac{1}{\rho\left(n_1^2 - Q_{0r} - n_m^2\right)^{1/2}}. \quad (33)$$

The complex n_{eff} is now obtained from (25), (26), and (33) and written in the usual form:

$$n_{\text{eff}} = \left(n_{\text{eff}}'^2 + jn_{\text{eff}}''^2\right)^{1/2} \quad \text{and} \quad \beta = kn_{\text{eff}}. \quad (34)$$

III. Numerical Solution of the Wave Equation

The wave equation (3) with $n^2(z)$ given by (1) is solved numerically by using the central difference formula

$$\Psi(z+\Delta z) = 2\Psi(z) - \Psi(z-\Delta z) - k^2\left[n^2(z) - n_{\text{eff}}^2\right]\Psi(z)(\Delta z)^2 \quad (35)$$

where Δz is a small increment in the depth dimension. Since $n^2(z)$ undergoes a sharp change at $z=0$, the above scheme is applied for $z>0$. In order to facilitate this, we use the boundary conditions of TM modes and note that TE mode results are obtained by making $\rho = 1$. We first designate the solution in the region $z<0$ by Ψ^- and in the region $z>0$ by Ψ^+. According to the boundary conditions, we have

$$\Psi^+(0) = \frac{n_m}{n_1}\Psi^-(0) \quad (36)$$

$$\frac{d}{dz}\Psi^+(0) = \frac{n_1}{n_m}\frac{d}{dz}\Psi^-(0). \quad (37)$$

By utilizing a Taylor series expansion, we write

$$\Psi^+(0+\Delta z) = \Psi^+(0) + \Delta z\frac{d\Psi^+(0)}{dz}. \quad (38)$$

From (36) and (37), we have

$$\Psi^+(\Delta z) = \frac{n_m}{n_1}\Psi^-(0) + \Delta z\frac{n_1}{n_m}\frac{d}{dz}\Psi^-(0). \quad (39)$$

The right-hand side of the above equation may be evaluated with the aid of (16), in which, for convenience, the arbitrary constant B is taken to be n_1/n_m, giving

$$\Psi^+(\Delta z) = \frac{n_m}{n_1}\Psi^-(0) + \Delta z\left(\frac{n_1}{n_m}\right)^2\theta = 1 + \Delta z\rho\theta \quad (40)$$

from which it is seen that $\Psi^+(0) = 1$.

Initial values for the iterative scheme of (35) are provided by $\Psi^+(0)$ and $\Psi^+(\Delta z)$ according to (36) and (40), respectively, and solutions obtained when convergence is assured. The efficiency of the scheme is facilitated by a good estimation of the value of n_{eff} for each mode and, hence, also the value of θ in (40). This estimate is calculated with the aid of (25), (26), and (33).

IV. Numerical Results and Discussion

Values of the propagation constants, as given by (25), (26), (33), and (34), are compared with those obtained numerically by the scheme of Section III. The waveguide parameters in all cases are $n_1^2 = 4.9665$, $n_2^2 = 4.8469$, $n_m^2 = -10.3 - j1.0$, corresponding to Ti-diffused $LiNbO_3$ and gold cladding at $\lambda = 0.6328$ μm. Values of β for the first three TE and TM modes are shown in Table I. It is noted that the labeling of TM modes in metal-clad waveguides may be confusing because of the existence of the surface plasma wave. This question is discussed in [3], and our TM mode labeling is consistent with that used in this reference. It is seen from Table I that the analytical and numerical results are in good agreement for both the β' and β''.

The accuracy of a simplified model in which only the first two terms of the Taylor series expansion of the Gaussian profile are

TABLE I
VALUES OF THE COMPLEX PROPAGATION CONSTANTS OF THE METAL-CLAD WAVEGUIDE WITH GAUSSIAN INDEX PROFILE

a_z in (μm)	Analytical values of β'	Numerical values of β'	Analytical values of β"	Numerical values of β"
		TE_0 Mode		
2	22.02136	22.02452	0.79304(-4)	0.75740(-4)
3	22.05474	22.05636	0.46128(-4)	0.44834(-4)
4	22.07221	22.07324	0.30965(-4)	0.30299(-4)
7	22.09546	22.09590	0.13952(-4)	0.13753(-4)
10	22.10501	22.10527	0.08309(-4)	0.08215(-4)
15	22.11255	22.11269	0.04582(-4)	0.04541(-4)
		TE_1 Mode		
2	21.90303	21.91598	0.90405(-4)	0.71710(-4)
3	21.96828	21.97289	0.57779(-4)	0.52999(-4)
4	22.00435	22.00676	0.40620(-4)	0.38692(-4)
7	22.05437	22.05518	0.19401(-4)	0.19022(-4)
10	22.07558	22.07608	0.11823(-4)	0.11675(-4)
15	22.09258	22.09280	0.06636(-4)	0.06581(-4)
		TE_2 Mode		
2	-	-	-	-
3	21.89384	21.90764	0.60074(-4)	0.45970(-4)
4	21.94361	21.94976	0.44303(-4)	0.39135(-4)
7	22.01576	22.01730	0.22470(-4)	0.21638(-4)
10	22.04740	22.04811	0.14018(-4)	0.13736(-4)
15	22.07317	22.07350	0.08111(-4)	0.07921(-4)

a_z in (μm)	Analytical values of β'	Numerical values of β'	Analytical values of β"	Numerical values of β"
		TM_0 Mode		
2	22.02136	22.01726	0.32207(-3)	0.31794(-3)
3	22.05474	22.05205	0.18761(-3)	0.18924(-3)
4	22.07221	22.07033	0.12604(-3)	0.12789(-3)
7	22.09546	22.09459	0.05685(-3)	0.05783(-3)
10	22.10501	22.10449	0.03387(-3)	0.03443(-3)
15	22.11255	22.11226	0.01869(-3)	0.01896(-3)
		TM_1 Mode		
2	21.90303	21.90932	0.36524(-3)	0.27884(-3)
3	21.96828	21.96789	0.23411(-3)	0.21442(-3)
4	22.00435	22.00510	0.16485(-3)	0.15820(-3)
7	22.05437	22.05337	0.07891(-3)	0.07839(-3)
10	22.07558	22.07491	0.04813(-3)	0.04818(-3)
15	22.09258	22.09218	0.02704(-3)	0.02716(-3)
		TM_2 Mode		
2	-	-	-	-
3	21.89384	21.90357	0.24260(-3)	0.17890(-3)
4	21.94361	21.94608	0.17931(-3)	0.15639(-3)
7	22.01576	22.01525	0.09124(-3)	0.08806(-3)
10	22.04740	22.04681	0.05700(-3)	0.05616(-3)
15	22.07317	22.07275	0.03261(-3)	0.03246(-3)

retained is of interest. In this case, the Gaussian profile becomes parabolic and the complex expression of n_{eff}^2 is obtained from (25), (26), and (33) by making $C_1 = C_2 = 0$. We thus have

$$n_{\text{eff}}'^2(\text{parabolic}) = n_1^2 - \frac{(2\eta+1)\, n_1\sqrt{2\Delta}}{a_z k} \tag{41}$$

where

$$\Delta = \frac{n_1^2 - n_2^2}{2n_1^2} \tag{42}$$

and

$$n_{\text{eff}}''^2(\text{parabolic}) = \frac{4}{\sigma}\left(\frac{n_0\sqrt{2\Delta}}{a_z k}\right)^{3/2} \text{Im}\left[\frac{1}{\rho\left(n_{\text{eff}}'^2 - n_m^2\right)^{1/2}}\right]. \tag{43}$$

Equations (41) and (43) are the same as those in [7] obtained for the parabolic model. Examination of (25) shows that for $n_{\text{eff}}'^2$, the Gaussian model tends to the parabolic model in a manner dependent on the mode order and the diffusion depth. For any particular mode, the two models become similar when a_z is large enough for the mode to be well guided. This condition is also true for $n_{\text{eff}}''^2$ given by (33) and (43). The mode attenuation increases with mode order in contrast to the mode attenuation in waveguides with linear [5] and exponential [6] profiles. In addition, the attenuation of TM modes is approximately an order of magnitude greater than that of TE modes.

ACKNOWLEDGMENT

The authors would like to thank the University of Petroleum & Minerals for providing the facilities and M. K. Butt for the manuscript.

REFERENCES

[1] S. J. Al-Bader and H. A. Jamid, "Comparison of absorption loss in metal-clad optical waveguides," *IEEE Trans. Microwave Theory Tech.*, vol. MTT-34, pp. 310–314, Feb. 1986.

[2] E. M. Garmire and H. Stoll, "Propagation losses in metal-film-substrate optical waveguides," *IEEE J. Quantum Electron.*, vol. QE-8, pp. 763–766, Oct. 1972.

[3] A. Reisinger, "Characteristics of optical guided modes in lossy waveguides," *Appl. Opt.*, vol. 12, pp. 1015–1025, May 1973.
[4] I. P. Kaminow, W. L. Mammel and H. P. Weber, "Metal-clad waveguides: Analytical and experimental study," *Appl. Opt.*, vol. 13, pp. 396–405, Feb. 1974.
[5] M. Masuda, A. Tanji, Y. Ando, and J. Koyama, "Propagation losses of guided modes in an optical graded-index slab waveguide with metal cladding," *IEEE Trans. Microwave Theory Tech.*, vol. MTT-25, pp. 773–776, Sept. 1977.
[6] T. Findakly and C. L. Chen, "Diffused optical waveguides with exponential profile: Effects of metal-clad and dielectric overlay," *Appl. Opt.*, vol. 17, pp. 469–474, Feb. 1978.
[7] S. J. Al-Bader, "Ohmic loss in metal-clad graded index optical waveguides," *IEEE J. Quantum Electron.*, vol. QE-22, pp. 8–11, Jan. 1986.
[8] R. V. Schmidt and I. P. Kaminow, "Metal-diffused optical waveguides in $LiNbO_3$," *Appl. Phys. Lett.*, vol. 25, pp. 458–460, Oct. 1974.
[9] T. Suhara, Y. Handa, H. Nishihara, and J. Koyama, "Analysis of optical channel waveguides and directional couplers with graded-index profile," *J. Opt. Soc. Am.*, vol. 69, pp. 807–815, June 1979.
[10] I. Savalinova and E. Nadjakov, "Modes in diffused optical waveguides (parabolic and Gaussian models)," *Appl. Phys.*, vol. 8, pp. 245–290, 1975.
[11] J. F. Lotspeich, "A perturbation analysis of modes in diffused optical waveguides with Gaussian index profile," *Opt. Commun.*, vol. 18, pp. 567–572, Sept. 1976.
[12] Y. Ayant, G. H. Chartier, and P. C. Jaussaud, "Étude a l'aide de l'optique integrée des processus de diffusion et d'echange d'ions dans un verre alcalin," *J. Phys.*, vol. 38, pp. 1089–1096, Sept. 1977.
[13] A. Gedeon, "Comparison between rigorous theory and WKB-analysis of modes in graded index waveguides," *Opt. Commun.*, vol. 12, pp. 329–332, Nov. 1974.
[14] J. Janta and J. Ctyrok'y, "On the accuracy of WKB analysis of TE and TM modes in planar graded-index waveguides," *Opt. Commun.*, vol. 25, pp. 49–52, Apr. 1978.
[15] G. B. Hocker and W. K. Burns, "Modes in diffused optical waveguides with arbitrary index profile," *IEEE J. Quantum Electron.*, vol. QE-11, pp. 270–276, 1975.
[16] C. J. Mullin, "Solution of the wave equation near an extremum of the potential," *Phys. Rev.*, vol. 92, pp. 1323–1324, 1953.
[17] D. E. Muller, "A method for solving algebraic equations using an automatic computer," *MTAC*, vol. 10, pp. 208–215, 1956.

A Novel Low-Noise Downconverter System Using a Microstrip Coupled Transmission-Mode Dielectric Resonator

MARY P. MITCHELL, STUDENT MEMBER, IEEE, AND
G. R. BRANNER, MEMBER, IEEE

Abstract—**A low-noise downconverter system for microwave downlink applications is presented. Although most downconverters with an internally generated local oscillator have been designed utilizing MESFET's and DGFET's, the circuit described herein uses a silicon bipolar Darlington pair as its active device and a dielectric resonator for feedback. Downconverters of the latter type have been realized with noise figures as low as 4.57 dB and conversion gains of 7 dB over an intermediate frequency range from 0.6 to 1.8 GHz.**

I. Introduction

There is currently an increasing interest in downconverter circuits which can be employed in low-noise receiver applications such as those found in commercial radio links, satellite broadcasting systems, and Doppler detectors.

Manuscript received May 12, 1986; revised September 8, 1986.
The authors are with the Department of Electrical and Computer Engineering, University of California, Davis, CA 95616. G. R. Branner is also with Avantek, Inc., Santa Clara, CA.
IEEE Log Number 8714406.

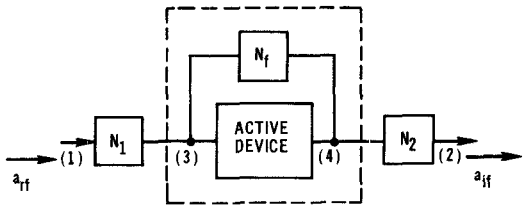

Fig. 1. Circuit configuration.

The application of single- and dual-gate GaAs MESFET's as downconverters has been reported previously [1]–[4] for frequencies in the *X*-band region. In addition to their advantage of simplicity, these devices have been shown to provide adequate conversion gain and IF bandwidth; however, their noise performance has been found to be a source of concern.

The objective of the effort reported in this paper was to develop a downconverter operating over the 3.7 to 4.2 GHz downlink band which would afford a simple, compact, and easy-to-construct design.

The design is unique in the sense that it utilizes a bipolar Darlington pair amplifier as its active device and dielectric resonator as feedback to provide a source of stable internally generated local oscillator signal power. Additionally, a uniquely synthesized diplexer circuit was developed for the output which provides a wide-band response over the 0.6 to 1.8 GHz intermediate frequency range used.

Design aspects of the downconverter and its circuit description and construction are given in Sections II and III. Experimental results are reported upon in Section IV.

II. Design Considerations

Several fundamental circuit configurations were investigated for the downlink receiver application being considered. A feedback-type structure was selected based on the system constraints involved and a desire for simplicity. This configuration is illustrated in Fig. 1. In this system, the RF signal a_{rf} is injected into port 1, mixed with an internally generated local oscillator (LO) signal created in the feedback device located between ports 3 and 4, and the resultant IF signal is extracted at port 2.

The basic function of networks N_1 and N_2 is to provide for signal matching and filtering at the input, and diplexing and matching at the output of the system. In the downconverter described here, these circuits are composed of passive microstrip elements and chip capacitors.

Several fundamental feedback arrangements may be employed to obtain the internally generated LO power required. These include series, parallel, or reflective feedback. Due to its temperature stability, compactness, tunability, and simplicity, a dielectric-resonator-based design was selected to perform this function [5]. Although this portion of the circuit could be realized with the dielectric resonator placed at either the input [6] or output [7] of the active device, the design developed employs the resonator as a parallel feedback element. This configuration has been found to possess numerous advantages over the others, such as ease of tuning [5], [6], [8].

The basic configuration of the dielectric-resonator feedback network employed in the local oscillator circuit is shown in Fig. 2(a). As illustrated in this figure, the circuit consists of a dielectric resonator placed between two curved microstrip lines. Thus, in this arrangement, there is magnetic coupling between the two